Simple and effective open switch fault diagnosis of single-phase PWM rectifier

Hu, Keting; Liu, Zhigang; Iannuzzo, Francesco; Blaabjerg, Frede

Published in:
Microelectronics Reliability

DOI (link to publication from Publisher):
10.1016/j.microrel.2018.06.023

Publication date:
2018

Document Version
Accepted author manuscript, peer reviewed version

Simple and Effective Open Switch Fault Diagnosis of Single-Phase PWM Rectifier

Keting Hu[a] , Zhigang Liu[a,*], Francesco Iannuzzo[b], Frede Blaabjerg[b]

[a] *School of Electrical Engineering, Southwest Jiaotong University, Chengdu, China*
[b] *Department of Energy Technology, Aalborg University, Aalborg, Denmark*

Abstract

In order to obtain lower harmonics distortion and higher power factors, single-phase pulse-width modulation (PWM) rectifiers are adopted in AC railway drive systems. Therefore, its reliability is of most importance with regards to the safe operation of the train. In this paper, a fault diagnosis method for open switch fault in single-phase PWM rectifier is proposed based on the switching system theory. It requires no additional sensor, nor extra operation states need to be set. Four observers which correspond to four kinds of open switch faults are utilized to detect and locate the faults. Real-time simulations are carried out to validate the effectiveness of this method.

Keywords: rectifier; open-switch fault; fault diagnosis

1. Introduction

Because of the higher power density and easier maintenance, AC motors have been widely applied in electrical drive systems, including the electrified high-speed railways, hybrid vehicles, etc. To power an AC motor, AC-DC-AC is the most common power supply solution, which consists of a rectifier, a DC-link and an inverter (see Fig. 1). Differently from the conventional diode rectifier, four-quadrant pulse width modulation rectifier (FQPWMR) is adopted in electrified high-speed railways, with the purpose of pursuing higher power factor, lower harmonic distortion and energy recovery [1]. According to [2], however, it is the weakest part of the drive system, which accounts nearly half of the faults from 2009 to 2013 in a Chinese high-speed railway. Therefore, the reliability of FQPWMR is of extreme importance.

Due to the vibration, humidity, high electrical and thermal stress, open-switch fault (OSF) and short-switch fault (SSF) of the Insulated Gate Bipolar Transistor (IGBT) are the most common failures in FQPWMR [3]. On the one hand, the SSF leads to an intense increase of the current, hardware protection is preferred to avoid the catastrophic consequences [4]. On the other hand, in the case of OSF, the system can

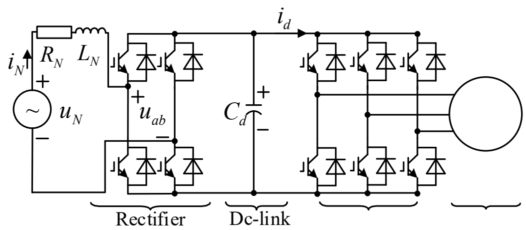

Fig. 1. Schematic of a AC drive system

still run for a while with higher stress on other devices before catastrophic failures occur, which recalls a fast fault diagnosis. At present, most efforts are focused on the three-phase converter, because it has a broad application [5, 6]. Only a few results are reported for OSF in FQPWMR. In [7, 8], it has been pointed out that it is quite challenging to identify the faulty IGBT pairs without additional sensors in single-phase PWM rectifiers. In order to overcome this problem, a particular state has been proposed to be applied to the rectifier for a short time, which can force the detection residual to get different values in case of faulty IGBT [9]. However, such a state can cause catastrophic short-circuit failure if such condition cannot be cleared on time. In [10], PWM pulse driven sampling method is proposed, which decouples the unidentified IGBT pairs on the

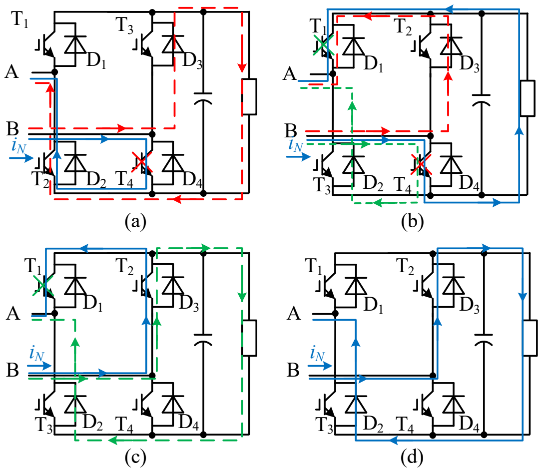

Fig. 2 Fault current path under control sequence (a) (0 1 0 1); (b) (1 0 0 1); (c) (1 0 1 0); (d) (0 1 1 0)

modulation level, making it able to distinguish all the four kinds of OSF. However, it is dedicated to the low switching frequency converter.

In this paper, a simple fault-current-observer based diagnosis, which is based on the switching system model (SSM) is proposed. By switching system theory, the grid current can be estimated by an open-loop observer. With the purpose of locating the fault, four fault current observers are generated, which can estimate the fault current under each fault by changing the control sequence of the SSM. When one of the estimated fault currents approaches the measured grid current, the faulty IGBT can be located without additional sensors or specific switching sequence.

2. Open switch fault analysis

Taking T_1 OSF and T_4 OSF as an example to illustrate how the OSFs effect the rectifier operation, and why the two IGBT pairs are challenging to be decoupled. Assume the grid current is positive when it flows into the rectifier and negative in the opposite direction. When the grid current is positive, it flows though the free-wheeling diodes D_1 and D_4 instead of the two corresponding IGBTs. Thus, the OSFs of T_1 and T_4 have no impacts on the converter.

When the grid current is negative, the current path is shown in Fig. 2. With the control sequence (0 1 1 0), the current path is same with the one under positive current situation, which indicates that the impacts of T_1 and T_4 OSFs on the rectifier is negligible. When the control sequence is (0 1 0 1),

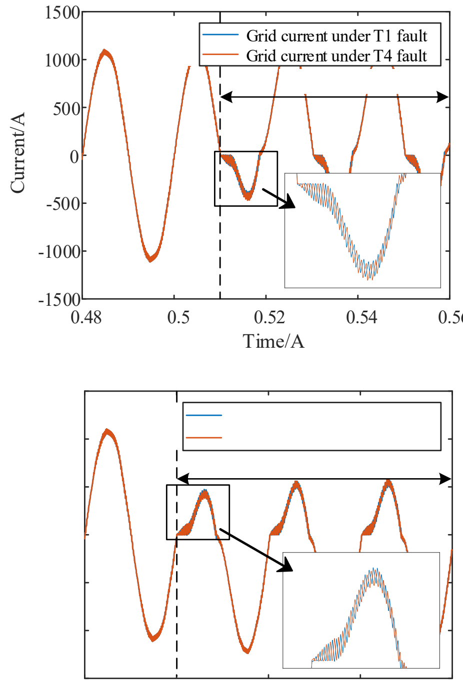

Fig. 3 Fault grid current under (a) T_1 and T_4 fault; (b) T_2 and T_3 fault

the current flows through T_4 and D_2 (see Fig. 2 (a)). As such, the voltage source is shorted and the current increases. In this case, T_4 OSF blocks the current path and it flows through D_3 and load, making the current decline. Meanwhile, as the current does not pass through T_1, T_1 OSF has not impacts on the rectifier. When the control sequence is (1 0 0 1), both T_1 and T_4 carry currents as Fig. 2 (b) shows. Therefore, either OSF on the two IGBTs will lead to current path change. Under normal condition, the current passes through T_4, load and T_1, makes both the DC capacitor and the voltage source charge the grid side inductor (see Fig. 1). Thus, the current increases intensely. However, if T_1 OSF or T_4 OSF occurs, the current will flow through D_2 or D_3 respectively. Then, there is only the voltage source charge the inductor, which causes the current rises slower. Finally, for the control sequence (1 0 1 0), the current paths before and after the T_1 OSF can be seen in Fig. 2 (c). The current decreases under the fault condition instead of rising in the normal condition. Meanwhile, the T_4 OSF cannot inflect the rectifier operation.

In overall, the T_1 OSF and T_4 OSF have the same impacts on the rectifier, which leads to the similar fault current for these two kinds of faults (see Fig. 3 (a)). It is also true for T_2 OSF and T_3 OSF, and

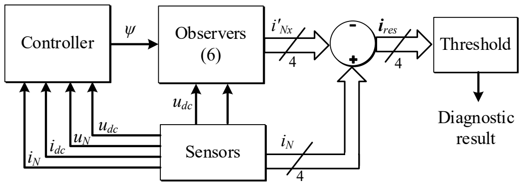

Fig. 4 Diagnostic scheme of the proposed method

the fault currents are shown in Fig. 3 (b). As a consequence, it is difficult to identify the faulty IGBT with only current analysis. In the next section, a simple diagnosis method will be introduced to overcome this problem.

3. Proposed diagnosis method

3.1. Switching system model

The FQPWMR can be described as

$$di_N/dt = A \times i_N + B_1 \times u_N + B_2 \times u_{ab} \qquad (1)$$

where $A = -R_N/L_N$, $B_1 = 1/L_N$, $B_2 = -1/L_N$, u_N is the grid voltage that can be obtained from the sensors, R_N and L_N are the leakage resistance and the leakage inductance that can be measured. However, the rectifier input voltage u_{ab} cannot be obtained directly. To describe u_{ab}, the SSM is introduced. All the operation modes of the rectifier and the corresponding values of u_{ab} are depicted in Table 1. As only three values (u_{dc}, 0, $-u_{dc}$) appear in all the modes, equation (1) can be transformed into the SSM as follows

$$di_N/dt = A \cdot i_N + B_1 \cdot u_N + B_\sigma(\psi) \cdot u_{dc},\ (\sigma \in \{1,2,3\}) \quad (2)$$

where $B_1(\psi)$=$-1/L_N$, $B_2(\psi)$=0, $B_3(\psi)$=$-1/L_N$. $B_\sigma(\psi)$ is performed on the system regards of the corresponding operation mode, which is driven by the control sequence

$$\psi = \Phi((\sigma_{k1},\tau_1), (\sigma_{k2},\tau_2),\ldots, (\sigma_{k18},\tau_{18})) \qquad (3)$$

where σ_{ki} represents the subsystem of one mode and τ_i is the corresponding working period. As u_{dc} can be sensed and ψ can be obtained from the control system, all the variables of the FQPWMR are known and the system can be described by the SSM.

3.2. Fault diagnosis method

With SSM (2), the open-loop grid current observer can be established as follows

Table 1 The value of u_{ab} under different operation modes

S1	S2	S3	S4	i_N	normal	T_1F	T_4F	T_2F	T_3F
0	0	0	0	<0	$-u_{dc}$	$-u_{dc}$	$-u_{dc}$	$-u_{dc}$	$-u_{dc}$
0	0	0	0	>0	u_{dc}	u_{dc}	u_{dc}	u_{dc}	u_{dc}
0	0	0	1	<0	0	0	$-u_{dc}$	0	0
0	0	0	1	>0	u_{dc}	u_{dc}	u_{dc}	u_{dc}	u_{dc}
0	0	1	0	<0	$-u_{dc}$	$-u_{dc}$	$-u_{dc}$	$-u_{dc}$	$-u_{dc}$
0	0	1	0	>0	0	0	0	0	u_{dc}
0	1	0	0	<0	$-u_{dc}$	$-u_{dc}$	$-u_{dc}$	$-u_{dc}$	$-u_{dc}$
0	1	0	0	>0	0	0	0	u_{dc}	0
0	1	0	1	<0	0	0	$-u_{dc}$	0	0
0	1	0	1	>0	0	0	0	u_{dc}	0
0	1	1	0	<0	$-u_{dc}$	$-u_{dc}$	$-u_{dc}$	$-u_{dc}$	$-u_{dc}$
0	1	1	0	>0	$-u_{dc}$	$-u_{dc}$	$-u_{dc}$	0	0
1	0	0	0	<0	0	$-u_{dc}$	0	0	0
1	0	0	0	>0	u_{dc}	u_{dc}	u_{dc}	u_{dc}	u_{dc}
1	0	0	1	<0	u_{dc}	0	0	u_{dc}	u_{dc}
1	0	0	1	>0	u_{dc}	u_{dc}	u_{dc}	u_{dc}	u_{dc}
1	0	1	0	<0	0	$-u_{dc}$	0	0	0
1	0	1	0	>0	0	0	0	0	u_{dc}

T_xF – The value of u_{ab} when T_x is faulty

$$di'_N/dt = A \cdot i'_N + B_1 \cdot u_N + B_\sigma(\psi) \cdot u_{dc},\ (\sigma \in \{1,2,3\}) \quad (4)$$

where i'_N is the observed grid current.

Then, the residual i_{res} can be obtained as Equation (5).

$$i_{res} = i_N - i'_N \qquad (5)$$

However, it is nearly impossible to locate the four kinds of potential faults with one residual which only has two directions, i.e., only two faulty IGBT pairs can be identified. This is another reason for the unidentified IGBT pairs. Aiming at this problem, the fault current observers are introduced. In the observer (4), B_σ is driven by ψ that represents the control sequence of the operation modes in Table 1. When an IGBT is open, it is stuck at on state. As a consequence, the control sequence will be changed, i.e. the corresponding command signal is equivalent to off in SSM. For example, if the control sequence is (0 1 0 1) to (**1** 0 0 1) when T_1 is faulty, the actual one performed on the system can be treated as (0 1 0 1) to (**0** 0 0 1), and this can be realized in the model by changing the switching sequence. Thus, four fault current observers can be derived as Equation (6), through transforming the normal control sequence into four faulty conditions respectively.

$$di'_{Nx}/dt = A \cdot i'_{Nx} + B_1 \cdot u_N + B_\sigma(\psi_x) \cdot u_{dc},\ (x \in \{1,2,3,4\}) \quad (6)$$

Where, i'_{Nx} represents the observed fault current

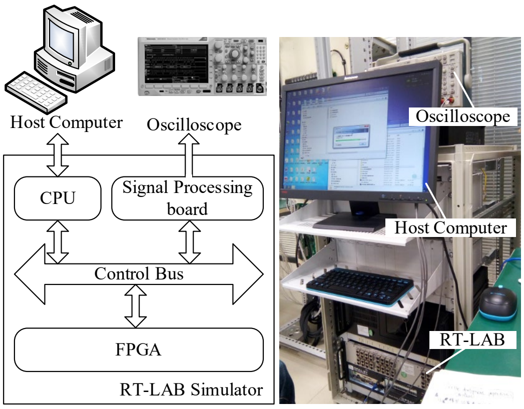

Fig. 5 Real time simulation platform

under T_x OSF, $B_\sigma(\psi_k)$ denotes the corresponding control sequence under T_x OSF.

With equation (5) and (6), the residual vector that contains four residuals can be derived as follows.

$$\boldsymbol{i}_{res} = [i_{res1}, i_{res2}, i_{res3}, i_{res4}]^{\mathrm{T}} \tag{7}$$

Each component in residual vector indicates one kind of fault in the rectifier. e.g., i_{res1} is an indicator for T_1 fault. If T_1 is open, the corresponding observed fault current i'_{Nx} will approach the actual grid current, and the indicator i_{res1} will approach zero, while the irrelevant indicators still remain a relatively large value. Therefore, all the fault conditions can be recognized by $\boldsymbol{i}_{res}$. Considering the modelling error and measurement error, a threshold is adopted to detect the fault, which is set as 500A according to experience. The overall diagnostic scheme is depicted as Fig. 4.

4. Real-time simulation

In order to validate the proposed diagnosis method, a real-time simulation is carried out in the RT-lab platform. It consists of a real-time simulator and a host computer, which is shown in Fig. 5. The simulation parameters are given in Table 2. The FQPWMR is controlled by the method presented in [11], while the load is a vector-controlled VSI-fed induction motor. The open-switch fault is emulated by removing the control signal. The T_1 fault, T_2 fault, T_3 fault, and T_4 fault are set at 0.5s, 1.5s, 2.5s, and 3.5s respectively and removed at 1s, 2s, 3s and 4s. The real-time simulation results of 125 rad/s speed and 1250 N·m torque, 150 rad/s speed and 1250 N·m torque, 150 rad/s speed and 1000 N·m torque, 125 rad/s speed and 1000 N·m torque of the load induction motor in the drive system are depicted in Fig. 6 (a), Fig. 6 (b), Fig. 6 (c) and Fig. 6 (d) respectively.

Table 2 Simulation parameters

Parameter	Symbol	Value
leakage resistance	R_N	0.13 Ω
leakage inductance	L_N	2.2 mH
Dc-link capacitor	C_d	2 mF
RMS grid voltage	u_N	1550 V
Dc-link voltage	u_{dc}	3000 V
Stator resistance	R_s	0.15 Ω
Stator leakage inductance	L_{ls}	1.42 mH
Rotor resistance	R_r	0.16 Ω
Rotor leakage inductance	L_{lr}	6 mH
Mutual inductance	L_m	25.4 mH
Rated voltage	U_{rate}	2750 V
Rated output power	P_{rate}	560 kW
Number of the pole pairs	n_p	2
Switching frequency	f_{sw}	2.5 kHz

It can be found that the values of all the residuals are more significant than the threshold under normal condition, even the load varies. Under all the different load conditions, the corresponding residual decreases sharply to the value that is smaller than the threshold within 0.03 second when an IGBT OSF occurs, while the remaining residuals stay outside of the residual zone, indicating the faulty IGBT is detected and identified. Though under some load conditions, the irrelevant residual will approach the threshold, its response time is much slower than that of the correct residual. Thus, the potential fault alarm can be eliminated by locking the diagnostic output once the fault is detected and identified.

5. Conclusion

An IGBT OCF in FQPWMR has been proposed in this paper. The OSF has been analysed firstly, and the difficulty of identifying the faulty IGBT pairs was explained. Then, the SSM of the rectifier was established, based on which four fault current observers were constructed. Next, by subtracting the real current with the observed current, the residual vector was generated. Finally, the faulty IGBTs were detected and identified through judging if the residuals were lower than the threshold, without additional sensors or particular states. Real-time simulation results validated the effectiveness of this method.

Acknowledgements

This study is partly supported by National

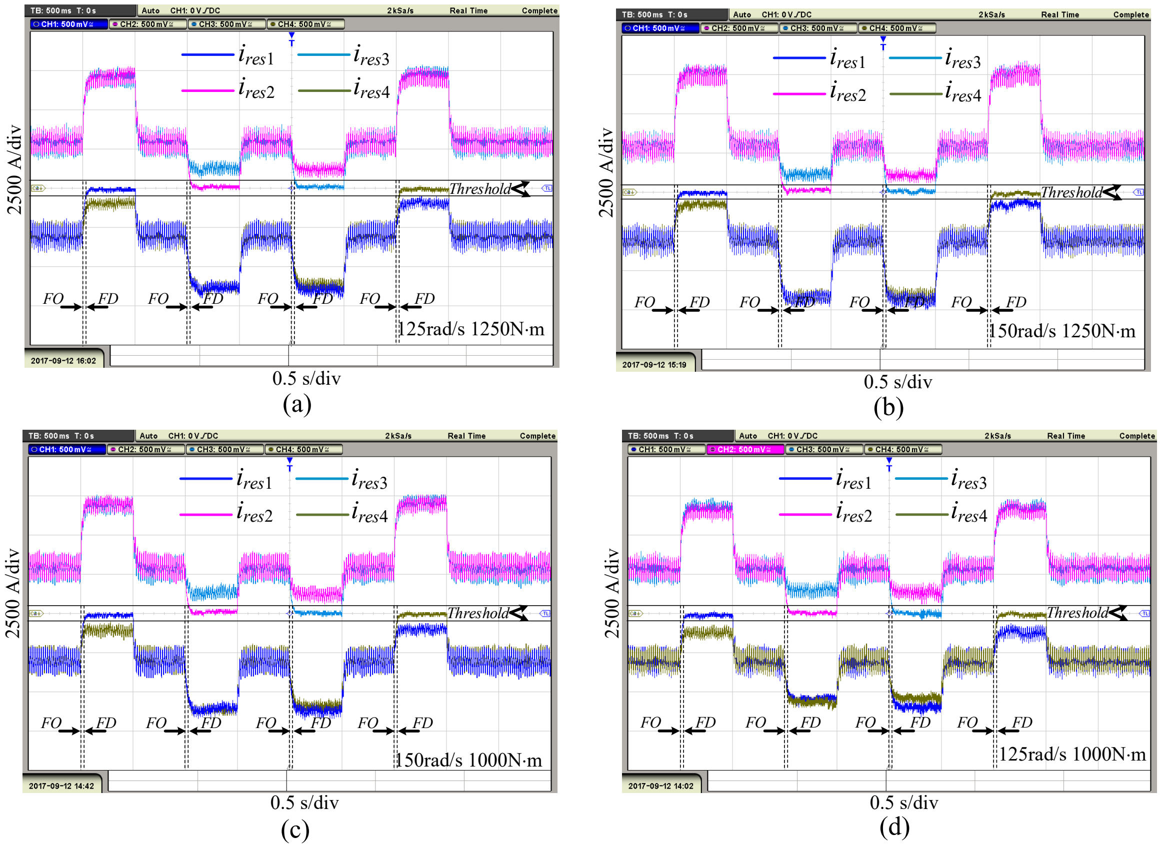

Fig. 6 Residuals when the load of the drive system under (a) 125 rad/s speed and 1250 N·m torque; (b) 150 rad/s speed and 1250 N·m torque; (c) 150 rad/s speed and 1000 N·m torque; (d) 125 rad/s speed and 1000 N·m torque; (FO means fault occurrence and FD indicates fault identified)

Nature Science Foundation of China (No. U1434203) and Sichuan Province Youth Science and Technology Innovation Team (No. 2016TD0012).

References

[1] A.B. Youssef, S.K. El Khil, I. Slama-Belkhodja. State observer-based sensor fault detection and isolation, and fault tolerant control of a single-phase PWM rectifier for electric railway traction, IEEE Trans. Power Electron. 28(2013) 5842-5853.

[2] B. Gou, Fault diagnosis and fault-tolerant control technology of railway electrical traction converter, Thesis, Southwest Jiaotong University, China, 2016.

[3] S. Yang, A. Bryant, P. Mawby, et al., An industry-based survey of reliability in power electronic converters, IEEE Trans. Ind. Appl. 47 (2011) 1441-1451.

[4] I. Jlassi, J.O. Estima, S.K. El Khil, et al., Multiple open-circuit faults diagnosis in back-to-back converters of PMSG drives for wind turbine systems, IEEE Trans. Power Electron. 30.5 (2015) 2689-2702.

[5] H. Oh, B. Han, P. McCluskey, et al., Physics-of-failure, condition monitoring, and prognostics of insulated gate bipolar transistor modules: A review, IEEE Trans. Power Electron. 30(2015) 2413-2426.

[6] U. Choi, F Blaabjerg, K. Lee, Study and Handling Methods of Power IGBT Module Failures in Power Electronic Converter Systems, IEEE Trans. Power Electron. 30.5 (2015) 2517-2533.

[7] A.M.S. Mendes, R. F. Rocha, A. J. Marques Cardoso, Analysis of a railway power system based on four quadrant converters operating under faulty conditions, Proc. IEMDC 2011, pp. 1019-1024.

[8] E. Craig, B.C. Mecrow, D.J. Atkinson, A.G. Jack, A fault detection procedure for single phase bridge converters, Proc. Power Electronics and Applications, 1993, pp. 466-471.

[9] B. Gou, X. Ge, S. Wang et al., An Open-Switch Fault Diagnosis Method for Single-Phase PWM Rectifier Using a Model-Based Approach in High-Speed Railway Electrical Traction Drive System, IEEE Trans. Power Electron. 31(2016) 3816-3826.

[10] X. Ge, J. Pu, Y. Liu, Online open-switch fault diagnosis method in single-phase PWM rectifiers, Electron. Lett. 51(2015) 1920-1922.

[11] H. Wang M. Wu, Simulation analysis on low-frequency oscillation in traction power supply system and its suppression method, Power System Technology, 39 (2015) 1088-1095.